ISSN 1070-3632, Russian Journal of General Chemistry, 2014, Vol. 84, No. 12, pp. 2375–2381. © Pleiades Publishing, Ltd., 2014.
Original Russian Text © K.S. Anisimov, A.A. Malkov, A.A. Malygin, 2014, published in Zhurnal Obshchei Khimii, 2014, Vol. 84, No. 12, pp. 1954–1961.

Mechanism of Thermal Oxidation of Silicon Carbide Modified by Chromium Oxide Structures

K. S. Anisimov, A. A. Malkov, and A. A. Malygin

St. Petersburg State Institute of Technology (Technical University), Moskovskii pr. 26, St. Petersburg, 190013 Russia
e-mail: malkov@lti-gti.ru

Received October 14, 2014

Abstract—Differential thermal analysis (DTA) and X-ray photoelectron spectroscopy (XPS) were used to study the oxidation of dispersed silicon oxide modified with chromium oxide structures by means of molecular layering, under linear heating in air to 1450°C. The mechanism of surface transformations of silicon carbide during its thermal oxidation was considered. It was shown that the oxidation resistance of the samples increased with increasing concentration of chromium in the surface film.

Keywords: silicon carbide, surface, modification, molecular layering, chromium oxides, silicon oxides, thermal treatment, mechanism of thermal oxidation

DOI: 10.1134/S1070363214120032

Silicon carbide is well known due to its the oxidation resistance provided by the silicon oxide film on its surface [1, 2]. Its semiconductor properties are of interest for the high-temperature electronic devices and heating elements creation [3]. One of the key tasks in the maintenance of products containing silicon carbide is stabilization and enhancement of its the oxidation resistance, which is first of all related to high-temperature electrical heaters operated at temperatures up to 1500°C. According to [4], this task can be solved by molecular layering of chromium oxide structures on the silicon carbide surface. However, in [4] no consideration was given for the mechanism of enhancement of the oxidation resistance.

The aim of the present work was to analyze physicochemical transformations occurring in the system SiC–surface chromium oxide structures at temperatures above 1000°C and to study the effect of chromium concentration on the silicon carbide surface on the oxidation resistance of the material.

The thermal oxidation of silicon carbide with oxygen resulting in the formation of a silicon oxide film on the surface can be described by the overall reaction (1) [1, 5].

$$SiC(solid) + O_2(gas) > SiO_2(solid) + CO_x(gas). \quad (1)$$

The reaction (1) mass balance analysis shows that the thermal oxidation of silicon carbide should be accompanied by mass gain of the sample. Comparison of the oxidation mass gains (m_{To}) for the starting and modified silicon carbide samples (Table 1) reveals a decrease of mass gain for chromium-containing samples. Therewith, this effect is the stronger the higher chromium concentration on the surface. Thus, taking into account reaction (1) we can conclude that the observed correlation indicates an enhancement of the oxidation resistance of the silicon carbide samples in the series SiC–3CrO_xSiC–6CrO_xSiC.

Tentative estimation of the thickness of the silicon oxide film forming on the surface of a solid substrate during oxidation shows that it regularly decreases with increasing concentration of chromium in the starting sample (Table 1)

Gas chromatography shows that the amount of CO_2 released by oxidation of the modified sample is much smaller than the amount of CO_2 released by oxidation of the starting silicon carbide (140 and 820 μmol m^{-2} h^{-1}, respectively), which is consistent with the gravimetry data and provides evidence for the inhibiting effect of surface chromium oxide structures on thermal oxidation of silicon carbide.

X-ray photoelectron spectroscopy (XPS) was used to study the chemical compositions of the starting SiC and modified 6CrO_xSiC samples before and after oxidation under heating to 1450°C in air (Figs. 1 and 2,

Table 1. Effect of chromium concentration on the mass of modified silicon carbide samples under heating in the range 20–1450°C in air

Sample	Chromium content calculated as Cr_2O_3, wt %	m_{To}, wt %	Δm_{To}[a], wt %	h[b], nm
SiC	0	1.3	0	78.7
$3CrO_xSiC$	0.051	0.5	–0.8	30.2
$6CrO_xSiC$	0.102	0.2	–1.1	12.1

[a] $\Delta m_{To} = m_{To}n(CrO_xSiC) - m_{To}(SiC)$. [b] ($h$) Thickness of the SiO_2 film calculated from m_{To}.

Table 2). The resulting atomic concentrations and element ratios in the surface film are listed in Table 2. Analysis of the XPS spectra of the thermally oxidized SiC samples surface revealed some specific features of the thermal oxidation process. Comparison of the surface compositions before and after thermal oxidation shows

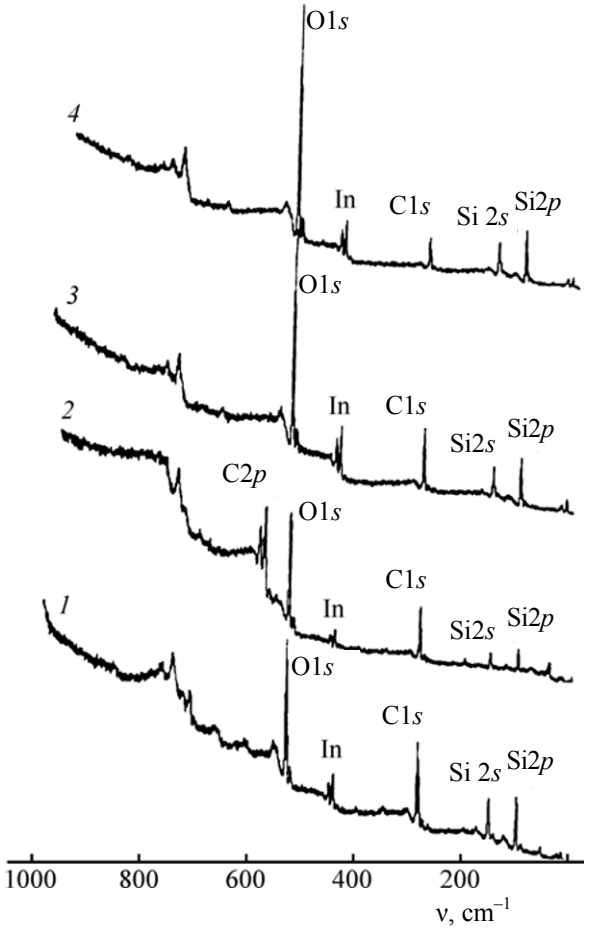

Fig. 1. XPS spectra of the (*1*, *3*) SiC and (*2*, *4*) $6CrO_xSiC$ samples (*1*, *2*) before and (*3*, *4*) after thermal oxidation.

that at the heat treatment in an oxidative atmosphere the relative content of carbon decreases and the relative content of silicon, oxygen, and O/Si atomic ratio increase (Table 2). Therefore, the relative atomic concentrations of silicon and oxygen in thermally oxidized modified samples are higher then in the starting silicon carbide. The lower surface carbon content in thermally oxidized samples is likely to be ascribed to the fact that the carbide phase in these samples is coated by the silicon oxide film being formed. The survey XPS spectra (Fig. 1) also revealed no Cr2*p* bands in thermally oxidized modified samples.

Analysis of local XPS bands (Fig. 2) made it possible to gain an insight into the changes in the chemical composition of surface structures in the course of heat treatment of the silicon carbide samples under study. In the Si2*p* spectral region (Fig. 2, curves *3* and *4*) of the XPS spectra of both samples we observe a strong change in the peak intensities of the silicon carbide and silicon bands: A well-defined maximum at 104 eV corresponding to the Si–O binding energy in SiO_2 and a much weaker maximum at 100.6 eV corresponding to the Si–C binding energy in silicon carbide and consistent with the band at 282.8 eV in the C1*s* region [6–9]. In the XPS spectra of the unheated samples, the silicon oxide maximum was observed at lower electron binding energies (~102 eV) (Fig. 2, spectra *1* and *2*), which appears to be due to the prevalence in the surface film of lower-oxidation-s tate silicon oxides [9]. Obviously, the exposure to high temperatures in an oxygen-containing medium forms a film of silicon oxide with silicon in a higher oxidation state. According to the review [5], the maximum thickness of the SiO_2 film on the SiC surface (~ 1 μm) is achieved after annealing for 20 h at 1200°C. At the same time, the spectra of oxidized samples show well-defined Si2*p* and C1*s* bands at binding energies characteristic of those in silicon carbide (100.2 and 282.6 eV, respectively) [7]. The observation of such bands suggests that the oxide film formed after heat treatment is either too thin or nonuniformly spread over the surface. The time of treatment at temperatures above 900°C was 2 h and above 1100°C, slightly more than an hour. Under such conditions the thickness of the silicon oxide film might reach at least 100 nm [5]. In this case, the XPS bands should not contain components assignable to silicon carbide, because the detection depth of the XPS analysis is no more than 8–10 nm [9]. The weight fraction of a uniform 8–10 nm

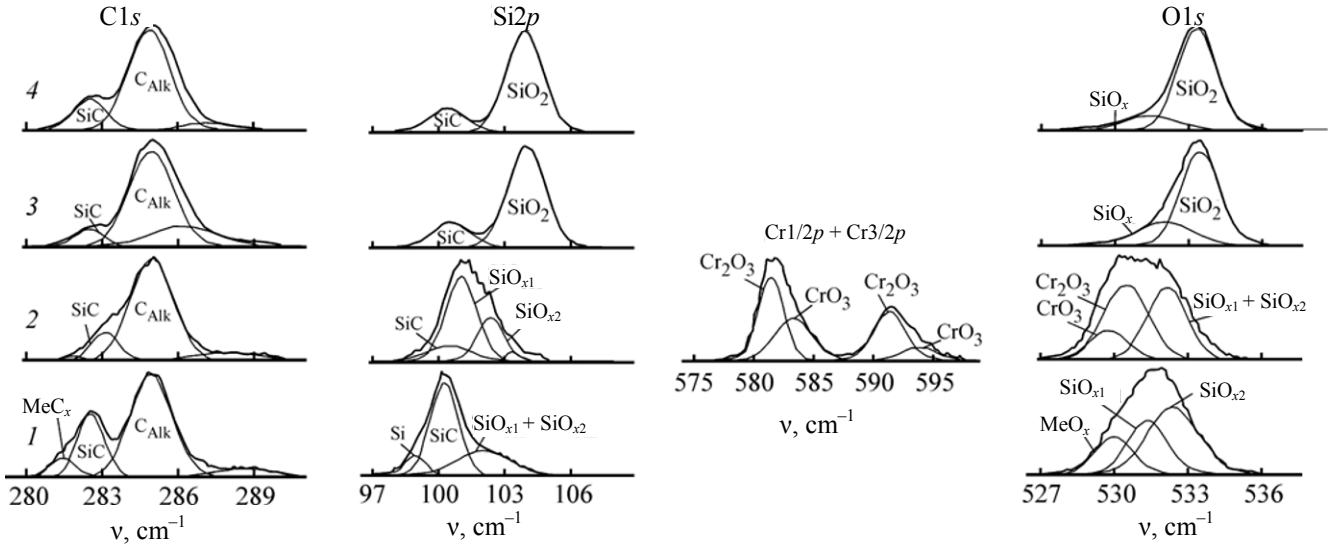

Fig. 2. Local C1*s*, Si2*p*, Cr2$p_{3/2}$, and O1*s* XPS spectra of (*1*, *3*) SiC and (*2*, *4*) 6CrO_xSiC samples (*1*, *2*) before and (*3*, *4*) after thermal oxidation.

thick oxide film that allows identification of the silicon and carbon atoms in the SiC film located beneath the oxide film was estimated, based on the silicon oxide film density (2.6 g/cm^3, quartz) [10] and particle size (25 × 25 × 50 μm) [11], at ~0.15 wt %. However, gravimetric measurements revealed a much larger weight gain in the starting silicon carbide after thermal oxidation (Table 1), which implies a large thickness of the resulting film.

It can be suggested that the formed silicon oxide film is nonuniform and includes parts where the film thickness is small enough to allow detection of bands associated with the SiC support (100.6 eV for Si2*p* 282.6 eV for C1*s* electrons). According to [5, 12], at temperatures above 1200°C, an active SiC oxidation mechanism is operative, when the SiC + O_2 and SiC + SiO_2 (oxide film) reactions first form intermediate gaseous oxides SiO and CO, and these oxides further react with oxygen in the gas phase to form a solid SiO_2, which deposits on the surface, and a gaseous CO_2, which goes away. Under such conditions, the thickness of the resulting silicon oxide film is controlled by the SiO oxidation rate. The described reaction mechanism is well consistent with the experimentally observed increase of the CO_2 concentration after the oxidation temperature has reached 1200–1300°C.

Table 2. Atomic composition of the surface of the starting and modified SiC samples before and after heating to 1450°C in air

Sample	Atomic concentration, %						Ratio	
	C1	O	Si	Cr	Fe	Cl	O/Si	O/Cr
Before heating								
SiC	46.07	29.28	21.28	–	3.26	–	1.38$^+$	–
6CrO_xSiC	34.62	39.74	10.76	13.27	–	1.62	1.84[a]	1.50[b]
1450°C								
SiC	38.31	39.33	22.36	–	–	–	1.76	–
6CrO_xSiC	25.82	47.57	26.61	–	–	–	1.78	–

[a] O/Si = (39.74 – 1.513.27)/10.76 = 1.84. [b] Stoichiometric ratio in Cr_2O_3.

It is notable that the positions of the principal components of the XPS bands (Fig. 2) and Si/C ratios (Table 2) are close after heat treatment of both samples (SiC and 6CrO_xSiC): After oxidation the relative content of silicon on the surface increases and the relative content of carbon decreases both in the modified and starting SiC samples. At the same time, the XPS spectra of the modified sample no longer contain the spin−orbital doublet corresponding to Cr2*p* electrons (Fig. 2), which can be due to several reasons.

First, our thermodynamic calculations showed that Cr_2O_3 is unlikely to be reduced to metal at 1450°C by silicon carbide or oxide with subsequent vaporization, especially in view of the high thermal stability of chromium (mp 1855°C [13]) (Table 3), On the other hand, according to published data the chromim-containing modifier can be removed from the surface due to high-temperature oxidation of Cr_2O_3 to CrO_3 and its subsequent vaporization. Berthod [14] observed this effect at the temperatures ≥1000°C with Cr_2O_3 protective coatings on the surface of chromium-containing alloys. However, even if chromium oxides are completely removed from the surface of SiC particles, the decrease in the weight gain observed in mofidied samples after their thermal oxidation does not coincide with the algebraic sum of the weight gain for the starting SiC sample and that for the sample with completely removed oxide modifiers.

In view of the aforesaid, we can suppose that the enhanced the oxidation resistance of the modified silicon carbide is not associated with the removal of chromium-containing structures from the sample. Probably, at high temperatures chromium atoms diffuse from the surface into the bulk of SiC particles to a depth more than 10 nm, which is the XPS depth limit. However, even of the diffusion process lasted indefinitely long and the chromium atoms were uniformly distributed over the bulk of SiC grains, the chromium concentration would be of about 4.2×10^{-2} mmol/cm^3. However, as judged from the depth distribution of chromium concentration calculated in [17], the maximum chromium concentration in the bulk of SiC up to a depth of about 10 nm at the temperature 1400°C and diffusion time 1 h (which is actually slightly longer than in our experiment) will be no more than 5.05×10^{-9} mmol/cm^3 (Table 4). This value is much lower than the sensitivity limit of the XPS instrument (0.1–1 at %). Thus, according to the calculations, the amount of chromium capable of diffusing into SiC is by about 7 orders of magnitude lower than the highest possible (4.2×10^{-2} mmol/cm^3), i.e. modifier diffusion into particle bulk can make some contribution to the removal of chromium from the surface of SiC during its oxidation, but this contribution is too low and does not explain why the Cr2*p* signal disappears from the XPS spectra of the thermally treated sample.

As known, the process of thermal oxidation of silicon carbide involves two stages with different mechanisms: passive (below 1200°C) and active (above 1200°C) [5, 12].

The schemes illustrating this process are shown in Fig. 3. At the passive oxidation stage (Fig. 3a), oxygen diffuses to the SiC–SiO_2 interface through a thin silicon oxide film. The oxidant reacts with SiC to form SiO_2 and CO. The silicon dioxide resulting from this reaction increases the total thickness of the silicon oxide film at the SiC–SiO_2 interface (i.e. from the internal side). Carbon monoxide diffuses to the surface, where it is oxidized with oxygen to CO_2 and released to the gas phase (Fig 3b). In the case of active oxidation (Fig. 3b), the greatest contribution is from direct reaction between SiC and SiO_2 giving volatile monoxides SiO and CO. These products diffuse to the grain surface, where they are oxidized to SiO_2 which is deposited onto the outer surface and CO_2 which is released to the environment. Thus, an important feature of active oxidation is that the silicon oxide film is built-up just on the outer side, i.e. the SiO_2 film formed by thermal oxidation at temperatures above 1200°C shields the surface chromium oxide structures, and this is the reason for the absence of the Cr2*p* signal in the XPS spectra.

As to the thermooxidative stability of the sample modified with chromium oxide structures, its increase at low temperatures (below 1200°C) is likely to be explained by a higher fraction of a higher SiO_2 oxide, as well as with a larger thickness of the oxide film [11], and, as a result, hindered diffusion of oxygen through this film. On the other hand, according to the observations in [18], the C/C–SiC composites coated with a film comprising Si, Mo, and Cr show enhanced the oxidation resistance. Therefore, after heat treatment of the composite under argon, which was required by the coating deposition conditions, the resulting protective film comprised the $MoSi_2$ and $CrSi_2$ silicides, and after subsequent oxidation at 1500°C for a few hours a SiO_2–Cr_2O_3 film formed. Zhang et al. ascribed the ob-served appreciable enhancement of the thermo-oxidative stability of the composite to the fact

Table 3. Free Gibbs energies for suggested reactions

Reaction	ΔG of the reaction at the temperature, kJ/mol			References
	298.15 K	1273 K	1673 K	
$SiO(g) + CrO_3(g) = SiO_2(s) + Cr_2O_3(s)$[a]	–707.11	–534.4	–446.88	[15], [16]
$2SiO(g) + O_2(g) = SiO_2(s)$[a]	–685.08	–478.8	–379.3	[16]
$4Cr_2O_3(s) + 3SiC(s) = 8Cr(s) + 3SiO_2(s) + 3CO_2$[b]	203.4	98.3	24.0	[15], [16]
$4CrO_3(s) + 3SiC(s) = 4Cr(s) + 3SiO_2(s) + 3CO_2$[b]	–900.6	–1086.9	–1171.8	[15], [16]
$2Cr_2O_3 + 3O_2 = 4CrO_3$[c]	32.29	484.9	697.5	[15], [16]

[a] Per 1 mole of SiO. [b] Per 1 mole of SiC. [c] Per 1 mole of Cr_2O_3.

Table 4. Chromium distribution at the diffusion into SiC particles at 1400°C at different annealing times

Time, s	Chromium concentration, mol/cm^3, at the depth, cm							
	2.0×10^{-7}	5.0×10^{-7}	1.0×10^{-6}	5×10^{-6}	5×10^{-5}	1×10^{-4}	1.5×10^{-4}	3×10^{-4}
1	8.1×10^{-11}	6.7×10^{-11}	3.4×10^{-11}	1.7×10^{-20}	0	0	0	0
600	2.2×10^{-9}	2.1×10^{-9}	2.16×10^{-9}	2.0×10^{-9}	5.0×10^{-11}	7.0×10^{-16}	0	0
3600	5.0×10^{-9}	5.0×10^{-9}	5.0×10^{-9}	5.0×10^{-9}	2.7×10^{-9}	4.2×10^{-10}	1.9×10^{-11}	1×10^{-18}

that chromium oxides stabilized the SiO_2 film at high temperatures due to vitrification and the increase in the crystallization temperature, which might increase the number of defects and facilitate diffusion in the bulk. Consequently, as the initiation temperature of the structural transformation increases, the diffusion rate under these temperature conditions tends to decrease. The oxidation rate at the active oxidation stage becomes constant for two reasons. The reagents at the passive oxidation stage are silicon carbide and oxygen. The concentration of oxygen at the SiC/SiO_2 interface increases with temperature due to enhanced diffusion, and this is responsible for increasing oxidation rate in the first stage. In going to active oxidation, the prevailing reaction is the reaction between SiC and SiO_2 leading to CO and SiO which diffuse to the surface and are oxidized by air oxygen to SiO_2 and CO_2. Both reagents (SiC and SiO_2) are solids, and, consequently, their concentration in the reaction zone remains unchanged during the entire reaction irrespective of the temperature. Moreover, SiO_2 deposits from the gas phase due to the oxidation of SiO to SiO_2 by air oxygen, and the resulting film fills defects and hinders diffusion of the reaction products.

EXPERIMENTAL

Dispersed KZ 6 silicon carbide (State Standard 3647-80) was used. Synthesis of chromium oxide structures on its surface and analysis of the samples for chromium was performed as described in [11, 19]. The synthesized powders were labeled nCrO$_x$SiC, where n is the number of cycles of successive and alternating treatment of the substrate by CrO_2Cl_2 and C_2H_5OH (H_2O) vapors according to the molecular layering technique [11, 19].

The XPS spectra were measured on a PHI 5–400 spectrometer at the reaction chamber pressure of 10^{-8} mm. Samples were pressed into indium plates. Photoelectrons were excited by MgK_α radiation (1253.4 eV). The determination of electron binding energies included the correction of band positions to account for the electric charge accumulated on the surface of the sample. The C1s band of adventitious carbon (tabulated E_b 285.0 eV) was used as internal reference [7, 9]. Deconvolution of the XPS bands into components was performed using Mathcad 14 software. The band components were fitted by pseudo-Voigt profiles using automated least-squares

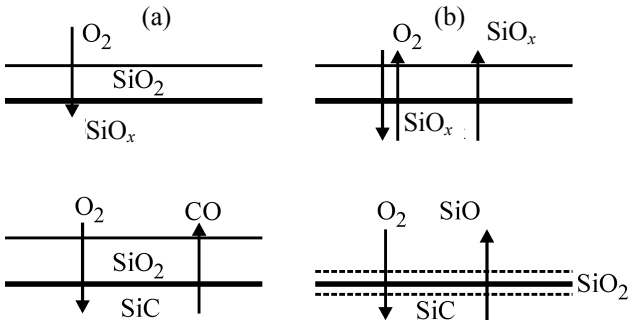

Fig. 3. Schematic representation of the (a) passive and (b) active SiC oxidation processes [5].

optimization of profile parameters for better fitting of the experimental data. Before deconvolution, fitting and background subtraction were performed for each band taking into account specifics of the XPS background. Differential thermal analysis was performed on a Paulik–Paulik–Erdey derivatograph (Hungary) in the range 20–1450°C at the heating rate 7.5°C/min in air with subsequent cooling of the oven and analysis of the solid products by XPS. The CO_2 content in the gas phase was performed on a Cromodam chromatograph (Setaram, France) with automated sampling every 3 min. The sensitivity of the CO_2 analysis was 0.03 vol %. The chromatographic CO_2 release curves were calibrated by the thermogravimetry and chromatography data obtained by burning of pet-coke which has a zero ash content in air. The thickness of the SiO_2 film formed during thermal oxidation was calculated by Eq. (2).

$$h = (m_{To}\rho_{SiC}\,abc)/[100\rho(SiO_2)\cdot 2(ab + bc + ac)]. \quad (2)$$

Here h is the SiO_2 film thickness, m; m_{To}, mass gain after thermal oxidation, wt %; ρ_{SiC}, density of SiC (3210 kg/m^3); $\rho(SiO_2)$, density of SiO_2 (2650 kg/m^3); and a, b, and c, grain sizes of KZ 6 silicon carbide, m (data from [11]).

Taking into account the low diffusion coefficient of chromium in silicon carbide (D_0 9.5 × 10^{-15} m^2/s, ΔE_a 81 kJ/mol) [14, 20] and, consequently, small depths of penetration of chromium atoms into SiC particles, the penetration thickness of chromium into the particles was estimated using the known equation for a semi-infinite plate under diffusion conditions [21].

$$C = Q/\{(\pi\cdot Dt)^{0.5}\exp[-(x^2)/(4Dt)]\}. \quad (3)$$

Here Q is the surface concentration of chromium, at/cm^2; x, penetration depth, cm; D, diffusion coefficient, cm^2/s; and t, diffusion time, s.

The diffusion coefficient was calculated by Eq. (4) [21].

$$D = D_0\cdot\exp(-\Delta E_g/RT). \quad (4)$$

Here D_0 is the pre-exponential factor, cm^2/s; ΔE_g, activation energy of the diffusion process, J/mol; and R, universal gas constant, J mol^{-1} K^{-1}.

The Q value was estimated from the chemical analysis for chromium and the specific surface of the samples.

Based on published and our present experimental data, we considered a two-stage mechanism of the thermal oxidation of the chromium-containing silicon carbide synthesized by the molecular layering technique. X-ray photoelectron spectroscopy was used to study the chemical composition and surface structure of thermally oxidized samples, which allowed us gaining insight into their transformations at different stages of thermal oxidation. It was found that the interface in the system "silicon carbide–silicon oxide–chromium oxide–outer silicon oxide" regularly shifts with tem-perature. As the thickness of the silicon oxide film on the outer grain surface increases, gradual shielding of the modifier and shifting of the outer silicon oxide–modifier oxide interface into the depth take place, and these reasons are responsible for the decrease of the modifier oxide concentration in the surface layer, revealed by the XPS analysis.

It was shown that chromium-containing silicon carbide samples show enhanced the oxidation resistance, and it is further enhanced as the surface concentration of chromium increases. Therewith, the two-stage mechanism of thermal oxidation is still operative. The enhancement of the oxidation resistance of SiC samples modified with chromium oxide structures can be explained by the fact that silicon is oxidized in the oxide film into SiO_2 at a low temperature in the first stage of the process and at a high temperature, by the formation of a protective glass film containing chromium oxide which increases the temperature of structural transformation and, consequently, accompanying defect formation.

ACKNOWLEDGMENTS

The work was financially supported in part by the Russian Science Foundation (project no. 14-13-00597) in the framework of the state order from the Ministry of Education and Science (no. 601).

REFERENCES

1. Gnesin, G.G., *Karbidokremnievye materialy* (Silicon Carbide Materials), Moscow: Metallurgiya, 1977.
2. Lebedev, A.A., Ivanov, A.M, and Strokan, N.B., *Fiz. Tekh. Poluprovodn*., 2004, vol. 38, no. 2, p. 129.
3. Willander, M., Friesel, M., Wahab, Q., and Straumal, B., *J. Mater. Sci. Mater. Electronics*, 2006, vol. 17. p. 1. DOI: 10.1007/s10854-005-5137-4.
4. Miroshnichenko, L.V., Malygin, A.A., and Kol'tsov, S.I., *Ogneupory*, 1985, no. 2, p. 225.
5. Benfdila, A. and Zekentes, K., *African Phys. Rev*., 2010, vol. 4, p. 25.
6. Bell, F.H. and Joubert, O., *J. Vac. Sci. Technol. B*, 1996, vol. 14, no. 4, p. 2493. DOI: 10.1116/1.588758.
7. Binner, J. and Zhang, Y., *J. Mater. Sci. Lett*., 2001, vol. 20, p. 123. DOI: 10.1023/A:1006734100499.
8. Libertino, S., Giannazzo, F., Aiello, V., Scandurra, A., Sinatra, F., Renis, M., and Fichera, M., *Langmuir*, 2008, vol. 24, p. 1965. DOI: 10.1021/la7029664.
9. Nefedov, V.I. and Cherepin, V.T., *Fizicheskie metody issledovaniya poverkhnosti tverdykh tel* (Physical Methods of Research of the Surface of Solids), Moscow: Nauka, 1983.
10. *Handbook of the Physicochemical Properties of the Elements*, Samsonov, G.V., Eds., Springer, 1968.
11. Anisimov, K.S., Malkov, A.A., Dubrovenskii, S.D., and Malygin, A.A., *Russ. J. Appl. Chem*., 2011, vol. 84, no. 8, p. 1299. DOI: 10.1134/S1070427211080015.
12. Jacobson, N.S. and Myers, N.L., *Oxid. Metals*, 2011, vol. 75, nos. 1–2. p. 1. DOI: 10.1007/s11085-010-9216-4.
13. Ripan, R. and Chetyanu, I., *Neorganicheskaya khimiya. Khimiya metallov* (Inorganic Chemistry. Chemistry of Metals), Moscow: Mir, 1972, vol. 2.
14. Berthod, P., *Oxid. Metals*, 2005. vol. 64, nos. 3–4, p. 235. DOI: 10.1007/s11085-005-6562-8.
15. *Kratkii spravochnik fiziko-khimicheskih velichin* (Concise Reference Book of Physicochemical Values), Ravdel', A.A. and Ponomareva, A.M., Eds., Leningrad: Khimiya, 1983.
16. Chase, M.W., Jr., *J. Phys. Chem. Ref. Data*, 1998, monograph 9, p. 1.
17. Takano, K., Nitta, H., Seto, H., Lee, C.G., Yamada, K., Yamazaki, Y., Sato, H., Takeda, S., Toya, E., and Iijima, Y., *Sci. Tech. Adv. Mater*., 2001, vol. 2, p. 381. DOI: 10.1016/S1468- 6996(01)00015-8.
18. Zhang, Yu-Iei, Li, He-Jun, Li, Ke-Zhi, Fei, Jie, and Zeng, Xie-Rong, *New Carbon Mater*., 2012, vol. 27, no. 2, p. 105. DOI: 10.1016/S1872-5805(12)60006-7.
19. Kol'tsov, S.I., Malygin, A.A., and Aleskovskii, V.B., *Zh. Obshch. Khim*., 1979, vol. 49, no. 9, p. 1936.
20. *http://www.chem.msu.su/Zn/Cr/print-CrO2Cl2.html.*
21. Gorelik, S.S. and Dashevskii, M.Ya., *Materialovedenie poluprovodnikov i dielektrikov* (Materials Science of Semiconductors and Dielectrics), Moscow: Mosk. Inst. Stali Splavov, 2003.